PHYSICAL REVIEW E VOLUME 57, NUMBER 3 MARCH 1998

Generalized smectic-hexatic phase diagram

Z. Kutnjak[1] and C. W. Garland[2]
[1]*Jozef Stefan Institute, P.O. Box 3000, 1001 Ljubljana, Slovenia 1001*
[2]*School of Science and Center for Material Science and Engineering, Massachusetts Institute of Technology, Cambridge, Massachusetts 02139*

(Received 4 August 1997)

The phase transitions from a smectic-*C* to a tilted hexatic phase are known to form a first-order transition line that terminates in an isolated critical point, beyond which there is supercritical evolution of bond-orientational order without a thermodynamic transition. Recent experiments strongly suggest that smectic-*A* (Sm-*A*) to hexatic-*B* (Hex-*B*) transitions are also first order, albeit in some cases very weakly so. A generalized smectic-hexatic phase diagram is proposed that unifies phase transitions involving tilted- and untilted-smectic and hexatic phases. Current information about Sm-*A*–Hex-*B* phase transitions is summarized and discussed in the context of *quasicritical* behavior. [S1063-651X(98)00103-2]

PACS number(s): 64.70.Md, 64.60.Fr

I. INTRODUCTION

The study of bulk hexatic phases, which exhibit long-range bond orientational order (BOO) but short-range in-plane positional order has been a very active field of research [1]. There are two aspects of this field: one involves untilted structures and the smectic-*A* (Sm-*A*) to hexatic-*B* (Hex-*B*) transition, and the other involves transitions from the tilted smectic-*C* (Sm-*C*) to either of two tilted hexatics that are denoted here as hexatic-*F* (Hex-*F*) and hexatic-*I* (Hex-*I*) [2]. The latter are usually denoted as smectic-*F* (Sm-*F*) and smectic-*I* (Sm-*I*) for historical reasons, but the notations Hex-*F* and Hex-*I* stress the essential BOO nature of these phases.

For symmetry reasons, Sm-*C*–Hex-*F* (or Hex-*I*) transitions must be first order, and this first-order transition line can terminate in an isolated critical point beyond which the BOO evolves supercritically without a thermodynamic transition [3,4]. Since there is a coupling between the tilt order parameter $\Theta = \theta\,\exp(i\phi)$ and the bond-orientational order parameter $\Psi = |\Psi|\exp(i6\psi)$, the tilt induces BOO in the Sm-*C* phase. The situation is analogous to that of the liquid-vapor transition in a simple fluid, except that the Sm-*C*–Hex-*F* (or Sm-*C*–Hex-*I*) critical point is not an Ising point but belongs to a new universality class [3]. Experimental evidence for this critical point has been observed calorimetrically for a mixture of 8SI+8OSI (methylbutylphenyl octylbiphenyl-carboxylate and its octyloxybiphenyl analog) [4] and from x-ray smectic layer thickness data for a mixture of (10)OSI+TB10A (terephthalbis-decylaniline) [5].

The Sm-*A*–Hex-*B* phase transition in untilted systems has been even more widely investigated. The thermal properties near such transitions have been extensively reviewed by Huang and Stoebe [6], and there are numerous structural studies (for example [7–9]). There are two types of Sm-*A*–Hex-*B* materials: those exhibiting a Sm-*A*–Hex-*B*–Cr-*E* phase sequence and those exhibiting a Sm-*A*–Hex-*B*–Cr-*B* sequence. Cr-*B* and Cr-*E* are three-dimensional (3D) plastic crystal-*B* and plastic crystal-*E*, and the latter has herringbone order (HBO) in the rotational orientations about the long axis of the liquid-crystal molecule. In the case of Hex-*B* phases that transform into Cr-*E* on cooling there is short-range HBO in the hexatic phase, while Hex-*B* phases that transform into Cr-*B* on cooling show no HBO fluctuations.

Since the BO order parameter Ψ which describes the six-fold azimuthal modulation has *XY* symmetry, the Sm-*A*–Hex-*B* transition was expected to exhibit 3D-*XY* critical behavior. However, this is not consistent with the experimental effective heat-capacity exponents $\alpha_{\mathrm{eff}} \simeq 0.5-0.65$ [6,10] or the BO order-parameter effective exponents $\beta_{\mathrm{eff}} \simeq 0.15-0.25$ [8,11]. In addition to this, recently reported heat-capacity results on two-layer films [12] do not agree with the expectations of 2D melting theory.

A number of theoretical models have been proposed to address the coupling between Ψ and tilt [3], HBO [13], positional density ρ [14,15], and smectic layer fluctuations u [16]. Although these models have yielded several successes—scaling of the harmonics in the tilted Hex-*I* phase of supercritical 8OSI [15,17] and the temperature variation of layer thickness in 46OBC (butyl-hexyloxybiphenyl-carboxylate) [7,14]—none has explained the detailed behavior near the Sm-*A*–Hex-*B* transition. Recent calorimetric studies of 65OBC [10] and 3(10)OBC [18] suggest that all Sm-*A*–Hex-*B* transitions are at least weakly first order but with very large pretransitional fluctuation C_p wings.

The purpose of this paper is to provide a general phase diagram that can act as a road map to unify the behavior of a wide variety of experimental smectic systems yielding Hex-*B*, Hex-*F*, and Hex-*I* hexatic phases. Section II presents the phase diagram and Sec. III contains a discussion of the current status of the Sm-*A*–Hex-*B* transition.

II. GENERALIZED SMECTIC-HEXATIC PHASE DIAGRAM

The global phase diagram shown in Fig. 1 is intended to provide an overview of smectic-to-hexatic transitions involving both Sm-*A* and Sm-*C* phases going to Hex-*B* and its

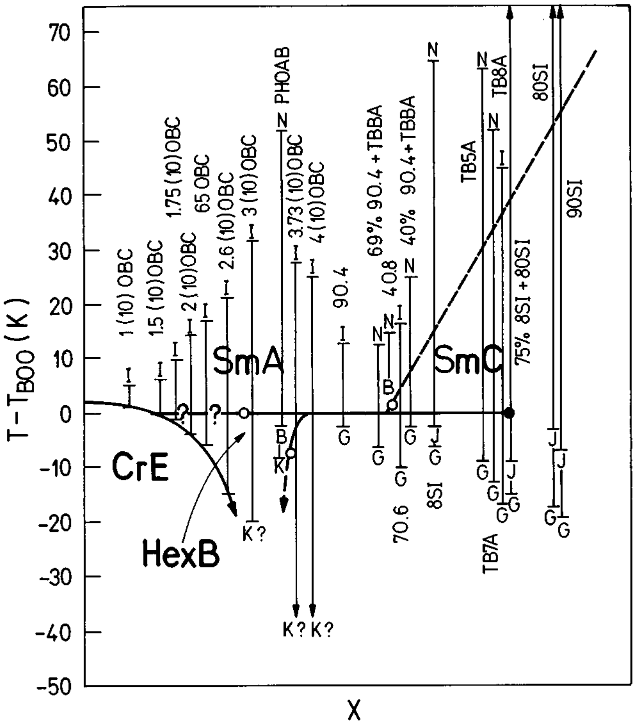

FIG. 1. Generalized phase diagram for smectic liquid crystals that form hexatic phases on cooling. The vertical scale is $T-T_{\mathrm{BOO}}$, where T_{BOO} is the temperature for the smectic-hexatic transition. The horizontal scale is a loosely defined general composition variable X (see text). The light vertical lines represent the range of stability for smectic and hexatic phases. The letters at the ends of these vertical lines denote the phases observed above the SmA and below the hexatic phase. Solid phase transition lines are first order and dashed lines are second order. In the lower right hexatic region, Hex-I is observed above the symbol J and at lower temperatures there is a Cr-J–Cr-G transition. In the absence of J, the symbol G indicates that the hexatic phase is Hex-F, which transforms into Cr-G at the indicated temperature.

tilted analogs Hex-F and Hex-I. In this diagram, the vertical axis is $T-T_{\mathrm{BOO}}$, where T_{BOO} is the smectic-hexatic transition temperature. The horizontal axis is a qualitative composition variable denoted as X. For homologous series such as $n(10)$OBC and TBnA, X is directly proportional to the value of n, where nonintegral values such as 3.73(10)OBC represent a binary mixture of two adjacent homologs [containing 73 wt % 4(10)OBC in this case]. The slope dT/dX of the Sm-A–Sm-C line is arbitrary, but the compounds exhibiting a Sm-C phase are plotted at X values that properly represent the temperature range of the Sm-C phase. The conventional names of the liquid crystals discussed in this paper are defined in terms of their proper chemical names and structural formulas in Table I. In both Figs. 1 and 2, the vertical lines are terminated at the top by the symbol N or I indicating which of these phases lies at temperatures above the position of the horizontal bar. At the bottom of many of the vertical lines here and in Fig. 2 the symbols B, G, J, and K denote the temperature at which the liquid crystal transforms on cooling into one of the plastic crystal forms Cr-B, Cr-G, Cr-J, or the rigid crystal Cr-K.

Figure 2 is a detailed view of the region between two triple points: the Sm-A–Hex-B–Hex-F (or Hex-I) and Sm-A–Sm-C–Hex-F (or Hex-I). In this region one sees a direct Sm-A–to–tilted-hexatic-phase transition. It should be noted that the freezing into a plastic crystal phase is strongly depressed near the Hex-B–Hex-F (or Hex-I) line. A possible explanation for this phenomenon is the presence of short-range Hex-F (or Hex-I) order in the Hex-B phase and short-range Hex-B order in the Hex-F (or Hex-I) phase, which could perturb the system enough to interfere with the nucleation of a plastic crystal phase.

The order of the transitions is indicated with dashed lines representing second-order transition lines and solid lines denoting first-order transition lines. Tricritical points are denoted by open circles and the Sm-C–Hex-I critical point is denoted by a filled circle. All known Sm-A–tilted-hexatic-phase transitions are first order. The behavior along the Sm-A–Sm-C line is well represented by ‘‘extended’’ Landau second-order transition theory [19], and a tricritical point is expected but not yet observed near the Sm-A–Sm-C–Hex-F triple point. (A Sm-A–Sm-C Landau tricritical point has, however, been observed in chiral systems [20].) As described in Sec. I, symmetry requires that Sm-C–tilted-hexatic-phase transitions must be first order, and this first-order line can terminate in a critical point [3]. Such a critical point has been observed in two systems [4,5] and *supercritical* Sm-C–tilted-hexatic behavior has been observed in 8OSI [4] and in 9OSI [21].

Another type of phase behavior must also be considered; the first-order freezing of a Sm-A, Sm-C, or Hex-B phase into the Cr-B plastic crystal phase. This can act to truncate the observation of tilted-hexatic phases and is indicated by the presence of the letter B for a few systems in Figs. 1 and 2. Examples of this freezing into Cr-B are the Sm-A–Cr-B transition in 4O.8 [22], the Sm-C–Cr-B transition in 4O.7 [23], and the Hex-B–Cr-B transition in PHOAB [24,25] and in many other recently studied materials [8,26–28] not included in Figs. 1 and 2. Indeed, the phase diagram for binary mixtures of 65OBC and 4O.8 [29] exhibits Sm-A, Hex-B, Cr-B, and Cr-E phases but no tilted-hexatic phases, and this diagram corresponds closely to the middle of Fig. 1 with the Cr-B phase region replacing that of the tilted hexatics and tilted plastic crystals. It should be noted that there do not appear to be any cases of transitions between Cr-B and the plastic crystals Cr-E, Cr-J, Cr-G, or any tilted hexatic phase.

III. DISCUSSION OF Sm-*A*–Hex-*B* TRANSITION

The principal concern in this section is the behavior of the Sm-A–Hex-B transition. Table II displays the basic information that is available for all the Sm-A–Hex-B systems known to us. When high-resolution heat-capacity data are available, they have been fitted with the power-law form

$$\Delta C_p = A^{\pm}|t|^{-\alpha_{\mathrm{eff}}}(1+D_1^{\pm}|t|^{\Delta}) + B_c^{\pm}, \tag{1}$$

where $\Delta C_p = C_p - C_p$ (background), $t=(T-T_c)/T_c$ is the reduced temperature, α_{eff} is the effective critical heat-capacity exponent, and $B_c^{\pm}$ is the contribution of the singular free energy to the regular heat-capacity behavior. For second-order transitions, $B_c^{+} = B_c^{-}$ is required and Δ is usually $\Delta_1 \simeq 0.5$. A step $\Delta B_c = B_c^{+} - B_c^{-} \neq 0$ is a signal of a first-order discontinuity. For some of the fits given in the litera-

TABLE I. Listing of liquid-crystal compounds by common name, chemical name, and structural formula. ϕ denotes a phenyl ring.

Common Name	Chemical name and formula
FLUn	1-(4′-alkyloxyphenylamino)-3-(4″-fluorophenyl)-propen-1-one-3 F-ϕ-COCH$=$CHNH-ϕ-OC$_n$H$_{2n+1}$
nmCOOBC	n-alkyl-4′-n-alkoyloxybiphenyl-4-carboxylate C$_m$H$_{2m+1}$-COO-ϕ-ϕ-COO-$C_n H_{2n+1}$
nO.m	N–(4-n-alkyloxybenzylidene)–4′-n-alkylaniline C$_n H_{2n+1}$O-ϕ-CH$=$N-ϕ-C$_m$H$_{2m+1}$
nmOBC	n-alkyl–4′-n-alkyloxybiphenyl–4-carboxylate C$_m$H$_{2m+1}$O-ϕ-ϕ-COO-C$_n$H$_{2n+1}$
nOSI	4–(2′-methylbutyl)phenyl–4′-n-alkyloxybiphenyl–4-carboxylate C$_n$H$_{2n+1}$O-ϕ-ϕ-COO-ϕ-CH$_2$-CH(CH$_3$)-C$_2$H$_5$
PHOAB	4-propionyl–4′-n-heptanoyloxy-azobenzene C$_2$H$_5$-CO-ϕ-N$=$N-ϕ-COO-C$_6$H$_{13}$
PIRn	1–(4′-alkyloxyphenylamino)–3[5″-(2″-methylpirydil)]-propen-1-one-3 H$_3$C-C$_6$H$_3$N-COCH$=$CHNH-ϕ-OC$_n$H$_{2n+1}$
RFLn	1-(4′-fluorophenylamino)–3(4″-alkyloxyphenyl)-propen-1-one-3 C$_n$H$_{2n+1}$O-ϕ-COCH$=$CHNH-ϕ-F
nSI	4-(2′-methylbutyl)phenyl-4′-n-alkylbiphenyl-4-carboxylate C$_n$H$_{2n+1}$-ϕ-ϕ-COO-ϕ-CH$_2$-CH(CH$_3$)-C$_2$H$_5$
TBnA	terephthal-bis-(4-n)-alkylaniline C$_n$H$_{2n+1}$-ϕ-N$=$CH-ϕ-CH$=$N-ϕ-C$_n$H$_{2n+1}$

ture (see Ref. [6] for a review), $\Delta B_c \equiv 0$ is maintained but Δ is taken to be 0.75. Such a fitting procedure produces a rounded pseudostep in B_c (see Refs. [10] and [18] for further details). X-ray data on the intensity of the sixfold azimuthal in-plane modulation C_6 can yield the effective critical exponent $\beta_{\rm eff}$ since

$$C_6 \sim \Psi \sim |t|^{\beta_{\rm eff}}. \tag{2}$$

For the 3D-XY model, $\alpha = -0.007$ and $\beta = 0.345$.

For the sake of completeness for the nmOBC series [6,30–34], Table II includes 4(10)OBC, which does not exhibit a Hex-B phase but undergoes a Sm-A–Hex-I transition [33]. Theory invoking Ψ-HBO coupling [13] has predicted a Sm-A–Hex-B tricritical point near the Sm-A–Hex-B–Cr-E triple point, but this has never been observed. The compound 1(10)OBC exhibits a direct Sm-A–Cr-E first-order transition, and a 1.75(10)OBC mixture seems to have a "second-order" Sm-A–Hex-B transition just 0.82 K above the Hex-B–Cr-E freezing transition [30]. Another theory invoking Ψ-position order coupling [15] has predicted a Sm-A–Hex-B tricritical point near the Sm-A–Hex-B–Cr-B triple point, but this also has not yet been observed (perhaps because work on Sm-A–Hex-B–Cr-B systems is very recent). There is an experimentally implied Sm-A–Hex-B–Hex-F (or Hex-I) triple point (shown in Figs. 1 and 2); such a triple point is consistent with the Defontaines-Prost theory, which couples Ψ to molecular tilt order [3]. That theory predicts a pair of tricritical points: one along the Sm-A–Hex-B line and one along the Hex-B–tilted-Hex (Hex-F or Hex-I) line. Observation of

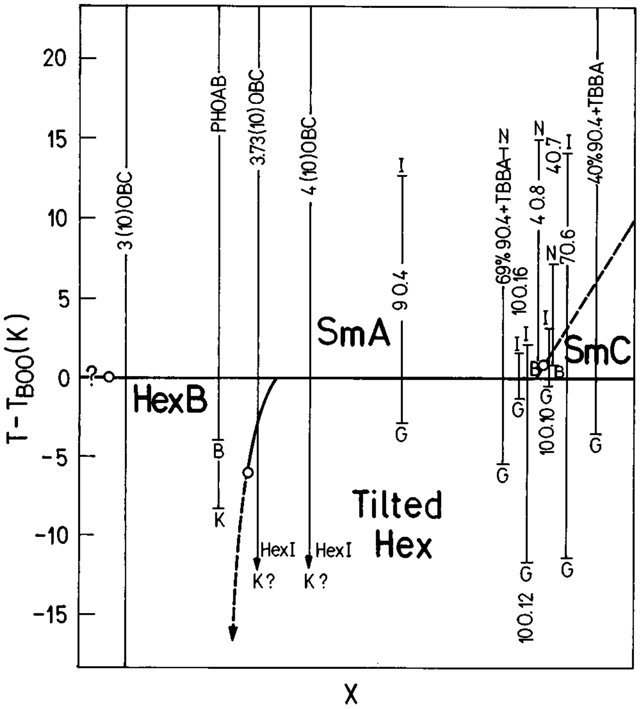

FIG. 2. Detailed view of the region between the Sm-A–Hex-B–Hex-F (or Hex-I) and Sm-A–Sm-C–Hex-F (or Hex-I) triple points. Solid phase transition lines are first order, dashed lines are second order, and the light vertical lines represent temperature ranges over which the Sm-A and hexatic phases are stable. All the tilted hexatic phases shown here are Hex-F except for 3.73(10)OBC and 4(10)OBC.

TABLE II. A summary of available heat-capacity and hexatic order-parameter information in the vicinity of the Sm-A–Hex-B transition. On further cooling, the Hex-B phase usually freezes via a first-order transition into Cr-E or Cr-B, but a rigid crystal Cr-X of unknown structure has also been observed. The fitting parameters for the excess heat capacity ΔC_p are T_c, α, A^-/A^+, and ΔB_c in J $\mathrm{K}^{-1}\,\mathrm{g}_{-1}$ where numerical values are available. The parameter uncertainties reported in the literature are ± 0.2 K in the absolute value of T_c, ± 0.03 for α_{eff} and ± 0.08 for A^-/A^+ unless otherwise stated. For $C_6(T) \propto |\Psi(T)|$ data, only the effective exponent β_{eff} is given. In the case of first-order transitions, T_c corresponds to the best estimate of the first-order T_1 transition temperature. A dash in the α_{eff}, A^-/A^+, and ΔB_c column indicates that power-law fitting of the data was tried and found impossible.

Compound[a]	Crystal phase	T_c (K)	Reported order of transition	Hysteresis[b] (mK)	Gap used in fit (mK)	Est. min. gap needed (mK)	α_{eff}	A^-/A^+	ΔB_c	β_{eff}	Refs.
45OBC	Cr-E	345.425	2nd[c]				0.48	1.00	yes[d]		[31]
65OBC	Cr-E	340.44	2nd		50	~50	0.60, 0.64	1.18	0.250		[31,32]
		340.85	very weak 1st	~1	75	~50	0.65 ± 0.05	1.09 ± 0.09	0.157	0.19	[10,11]
65OBC +10% 4O8	Cr-E	340.45	weak 1st	15	100	~120	0.49	1.22	yes		[32]
75OBC	Cr-E	337.525	2nd[c]				0.62	1.10	yes[d]		[31]
26OBC	Cr-E	373.17	2nd[c]				0.59	1.10	yes[d]		[6]
36OBC	Cr-E	348.54	2nd[c]				0.58	1.08	yes[d]		[31]
46OBC	Cr-E	340.41	2nd[c]				0.60, 0.49	1.25, 1.30	yes[d]		[6,31]
37OBC	Cr-E	344.14	2nd	cool	~40	~60	0.56	1.28	yes[d]		[31]
1.75(10)OBC	Cr-E	375.45	2nd	cool	~60	~78	0.58	0.97	yes[d]		[30]
2(10)OBC	Cr-E	367.82	2nd	cool	~60	~88	0.64, 0.67	1.10, 1.11	yes[d]		[30,31]
2.25(10)OBC	Cr-E	360.645	2nd	cool	~60	~100	0.58	1.04	yes[d]		[30]
2.6(10)OBC	Cr-E	350.77	2nd[c]	cool	~60		0.58	1.16	yes[d]		[30]
3(10)OBC	Cr-X	340.24(38)[e]	2nd	cool	60	~105	0.56, 0.59	1.33, 1.41	~0.18		[24,30,31,33]
		339.63	weak 1st	14.6	375	~260 coex.	0.68 ± 0.10	1.33 ± 0.1	0.200		[18]
3.05(10)OBC	Cr-X	339.0	1st?	cool		~100	0.76	1.61	yes[d]		[34]
3.73(10)OBC	Hex-I[f]–Cr-K	330.75	1st	cool	~260 coex.	~260	–	–	–		[33]
4(10)OBC	Sm-A–Hex-I[f]–Cr-K	~327.55	1st	cool	610 coex.		–	–	–		[33]
PHOAB	Cr-B	361.59	1st	cool	~320 coex.	~375	–	–	–		[24,25]
34COOBC	Cr-B	338.53	1st	cool	⩾150 coex.	~200	0.42, 0.87[g]		yes		[26]
54COOBC	Cr-B	328.56	1st	cool	~90 coex.		–	–	–		[27]
64COOBC	Cr-B	331.05	1st	cool	⩾140 coex.	~200	0.48, 0.76[g]		yes		[26]
RFL6	Cr-B		1st							0.15	[8]
FLU9	Cr-B										[8]
PIR5	Cr-B									0.25	[8]
PIR7	Cr-B	381.66	1st	340	200		0.15 ± 0.08	1.39	0.18	0.20	[8,28]
PIR9	Cr-B	385.38	2nd?	0	200		0.18 ± 0.08	1.06	?		[28]

[a] For nmOBC a fractional value of n means mixture; e.g. 1.75(10)OBC is a mixture of n=1 and n=2 compounds with 75 wt % of the latter.

[b] For most nmOBC compounds, only cooling data are available, but it is reported in Ref. [6] that there is no hysteresis greater than the resolution (~3 mK).

[c] No experimental data or details are available, just the fitting parameters given in a table in Refs. [6] and [31].

[d] The entry ''yes'' with this footnote indicates the qualitative presence of a step because fitting was carried out with Eq. (1) using $\Delta = 0.75$, $D_1^{\pm} \neq 0$, and $B_c^+ = B_c^-$. However, this empirical correction term mimics a step (see Refs. [10,18]). Unfortunately, Refs. [30–34] do not report $D_1^{\pm}$ values, but see footnote 17 in Ref. [30].

[e] The data close to T_c and the fit parameters differ somewhat for Refs. [24,30,33]; see Ref. [18] for further details.

[f] For the mixture of n=3 and n=4 with 73 wt % 4(10)OBC, the phase sequence in Sm-A–Hex-B–Hex-I–Cr-K. For pure 4(10)OBC, there is a direct Sm-A–Hex-I transition with no Hex-B phase.

[g] These C_p data were fit with $a^+ \neq \alpha^-$.

the latter is difficult since Hex-B–tilted-Hex lines seem to be steep (large dT/dX) and freezing into a rigid crystal phase can intervene. There are, however, Hex-B–Hex-F transition lines near Sm-C–Hex-F–Hex-B and Hex-B–Hex-F–Cr-G triple points [35,36], which have not yet been studied in detail.

Now let us review the present status of the Sm-A–Hex-B transition. Transitions that are described as probably first order have been reported previously in PHOAB [24,25] and 3.73(10)OBC [33], and definite first-order Sm-A–Hex-B character has been observed in 34COOBC, 64COOBC [26], 54COOBC [27], and PIR7 [28]. Except for 3.73(10)OBC, all of these systems exhibit the Sm-A–Hex-B–Cr-B sequence. Indeed, no second-order Sm-A–Hex-B transition is yet established in systems with the Sm-A–Hex-B–Cr-B sequence. PIR9 is the best presently known prospect [28] although the Hex-B range of 9.25 K in PIR9 is not large compared with those in many nmOBC compounds [30]. All Sm-A–Hex-B transitions in materials with the Sm-A–Hex-B–Cr-E sequence and 3(10)OBC, where the sequence is Sm-A–Hex-B–Cr-X (=Cr-K?), have been reported by the Huang group as second order with anomalous C_p exponents α_{eff} in the range 0.48–0.67 (see Table II and Ref. [6]). However, we believe that both 65OBC [10] and 3(10)OBC [18] exhibit weak first-order transitions with substantial pretransitional wings. In the case of 3(10)OBC, two-phase coexistence is clearly established and the assignment of first order instead of second order is easily incorporated into Figs. 1 and 2 by putting the Sm-A–Hex-B tricritical point slightly to the left of 3(10)OBC.

The greatest mystery is why a line of Sm-A–Hex-B transitions exhibit α_{eff} values that do not fit into any simple universality class but seem close to Gaussian tricritical ($\alpha=0.5$, $\beta=0.25$, and $\gamma=1$) or Gaussian tetracritical ($\alpha=\frac{2}{3}$, $\beta=\frac{1}{6}$, and $\gamma=1$). Huang and co-workers [6,30,31] have demonstrated that the width of the Sm-A phase range, i.e., $T_1(I\text{-}A)-T_c(A\text{–Hex-}B)$, and that of the Hex-$B$ range, $T_c(A\text{–Hex-}B)-T_1(\text{Hex-}B\text{–Cr-}E)$, have no systematic effect on the apparent critical Sm-A–Hex-B behavior. The latter result implies that Ψ-HBO coupling is irrelevant.

A recent high-resolution calorimetric study of 65OBC [10] shows that the Sm-A–Hex-B transition in this prototypical and best-studied hexatic compound is *very weakly* first order. The first-order character is small and subtle and would be very difficult to detect if the scan rate were too high. The proposed explanation of this result for 65OBC was *quasicritical* or *quasitetracritical* behavior based on a $|\Psi|^2$ (strain) coupling between the BO amplitude $|\Psi|$ and the *in-plane* positional strain [10]. Such an order-parameter strain (or density) coupling could generate a line of quasicritical points that would be second-order points in the absence of such coupling. Thus we propose that all Sm-A–Hex-B transitions are at least weakly first order with some smeared small latent heat effects rounding the C_p peaks, as is seen in essentially all Sm-A–Hex-B transitions that were previously described as second order. Thus we denote the Sm-A–Hex-B transition as *quasicritical* in the sense of Bergman and Halperin [37], who developed a strain coupling theory for the quasicritical behavior of a compressible Ising model. This is indicated in Figs. 1 and 2 by question marks along the transition line to the left of the putative Sm-A–Hex-B tricritical point. In the absence of this coupling, the first-order latent heat ΔH would decrease to zero at an isolated tricritical point and remain zero along the subsequent second-order line. However, a quasicritical system is always first order, with ΔH decreasing rapidly to a very small value but remaining nonzero. In such a situation, the pretransitional C_p wings should be dominated by the multicritical point rather than the underlying second-order fixed point [37]. See Ref. [10] for a further discussion of weakly first-order quasicritical Sm-A–Hex-B transitions. It should be noted that in Ref. [26] Mahmood *et al.* speculate that the Hex-B phase may be a fluctuation-induced phase sensitive to positional order. Thus they suggest that the relative scarcity of the Hex-B phase is due to the fact that either Cr-B or Cr-E can have a lower free energy and preempt the hexatic.

The presence of significant short-range positional order (in-plane correlational lengths $\xi_{\parallel}\sim200$ Å) in hexatic phases [7,8] is attested to by the very small C_p anomalies and tiny latent heats associated with the Hex-B–Cr-E, Hex$B$–Cr-B, Hex-F–Cr-G, and Hex-I–Cr-J first-order freezing transitions. Almost all the enthalpy associated with positional order develops very close to the smectic-hexatic transition, and the achievement of true long-range positional order is significant for x-ray or electron-diffraction studies but counts for little in thermal studies.

The utility of Figs. 1 and 2 is to provide a road map for considering all the coupling features that can play a role: Ψ coupled to HBO, tilt, Cr-B-like positional density, and in-plane positional density. Note that if we disregard the 3D positionally ordered plastic crystals Cr-E, Cr-B, Cr-G, and Cr-J for the moment and consider two order parameters—the tilt angle Θ and the hexatic BOO Ψ—there is a neat pattern [3,38]. Sm-A has $\Theta=\Psi=0$, Sm-C has $\Theta\neq0$, $\Psi\neq0$ and Ψ is very small, Hex-B has $\Theta=0$, $\Psi\neq0$, and Hex-F (or Hex-I) has $\Theta\neq0$, $\Psi\neq0$ and Ψ is large.

We do not claim that Fig. 1 is a universal phase diagram for all smectic-hexatic systems. As discussed at the end of Sec. II, there is a Sm-A–Hex-B–Cr-B alternative diagram in which the Sm-A–Hex-B transitions are clearly first order (with the possible exception of PIR9). In addition, recent studies show that THI-n homologs (thienyl-enaminoketone derivatives) exhibit Sm-C–Hex-F–Hex-B sequences and a Sm-C–Hex-F–Hex-B triple point [35], and JTH-n homologs (enaminoketone derivatives) exhibit the Sm-A–Hex-B–Hex-F–Cr-G sequence for several n and have a Hex-B–Hex-F–Cr-G triple point [36]. These results suggest that the Hex-B–tilted hexatic line can also be located much further to the right than in Fig. 1 (and with an opposite slope dT/dX). It should be noted that both these phase sequences are compatible with the Defontaines-Prost model [3].

ACKNOWLEDGMENTS

The authors wish to thank G. Nounesis and G. Iannacchione for helpful discussions. This work was supported in part by the National Science Foundation under Grant No. DMR 93-11853. One of the authors (Z.K.) wishes to acknowledge support from the Fulbright program and the Ministry of Science of Slovenia during a stay at MIT.

[1] P. G. deGennes and J. Prost, *The Physics of Liquid Crystals* (Clarendon, Oxford, 1993), pp. 547–551, and references cited therein.

[2] There is also a third tilted hexatic, the smectic-L (or hexatic-L) that will not concern us here.

[3] A. D. Défontaines and J. Prost, Phys. Rev. E **47**, 1184 (1993).

[4] H. Yao, T. Chan, and C. W. Garland, Phys. Rev. E **51**, 4585 (1995), and references cited therein.

[5] S. Krishna Prasad, D. S. Shankar Rao, S. Chandrasekhar, M. E. Neubert, and J. W. Goodby, Phys. Rev. Lett. **74**, 270 (1995).

[6] C. C. Huang and T. Stoebe, Adv. Phys. **42**, 343 (1993), and references cited therein.

[7] R. Pindak, D. E. Moncton, S. C. Davey, and J. W. Goodby, Phys. Rev. Lett. **46**, 1135 (1981); J. W. Goodby and R. Pindak, Mol. Cryst. Liq. Cryst. **75**, 233 (1981); S. C. Davey, J. Budai, R. Pindak, J. W. Goodby, and D. E. Moncton, Phys. Rev. Lett. **53**, 2129 (1984).

[8] E. Gorecka, L. Chen, S. Kumar, A. Krowczynski, and W. Pyzuk, Phys. Rev. E **50**, 2863 (1994); E. Gorecka, L. Chen, A. Lavrentovich, and W. Pyzuk, Europhys. Lett. **27**, 507 (1994).

[9] C.-F. Chou, J. T. Ho, S. W. Hui, and V. Surendranath, Phys. Rev. Lett. **76**, 4556 (1996), and references cited therein.

[10] H. Haga, Z. Kutnjak, G. Iannacchione, S. Qian, D. Finotello, and C. W. Garland, Phys. Rev. E **56**, 1808 (1997).

[11] C. Rosenblatt and J. T. Ho, Phys. Rev. A **26**, 2293 (1982); see footnote 14 in this paper.

[12] T. Stoebe, C. C. Huang, and J. Goodby, Phys. Rev. Lett. **68**, 2944 (1992); T. Stoebe and C. C. Huang, Phys. Rev. E **50**, R32 (1994); A. J. Jin *et al.*, Phys. Rev. Lett. **74**, 4863 (1995).

[13] R. Bruinsma and G. Aeppli, Phys. Rev. Lett. **48**, 1625 (1982).

[14] G. Aeppli and R. Bruinsma, Phys. Rev. Lett. **53**, 2133 (1984).

[15] A. Aharony, R. J. Birgeneau, J. D. Brock, and J. D. Litster, Phys. Rev. Lett. **57**, 1012 (1986).

[16] J. V. Selinger, J. Phys. (Paris) **49**, 1387 (1988).

[17] J. D. Brock *et al.*, Z. Phys. B **74**, 197 (1989).

[18] H. Haga and C. W. Garland, Phys. Rev. E **57**, 603 (1998).

[19] C. C. Huang and J. M. Viner, Phys. Rev. A **25**, 3385 (1982); M. Meichle and C. W. Garland, *ibid.* **27**, 2624 (1983).

[20] T. Chan, Ch. Bahr, G. Heppke, and C. W. Garland, Liq. Cryst. **13**, 667 (1993); H. Y. Lui, C. C. Huang, Ch. Bahr, and G. Heppke, Phys. Rev. Lett. **61**, 345 (1988).

[21] E. K. Hobbie, H. Y. Liu, C. C. Huang, and J. Liang, Phys. Rev. A **37**, 3963 (1988).

[22] K. J. Lushington, G. B. Kasting, and C. W. Garland, J. Phys. (Paris) Lett. **41**, L419 (1980).

[23] E. Bloemen and C. W. Garland, J. Phys. (Paris) **42**, 1299 (1981); R. J. Birgeneau *et al.*, Phys. Rev. A **27**, 1251 (1983).

[24] C. C. Huang, G. Nounesis, R. Geer, J. W. Goodby, and D. Guillon, Phys. Rev. A **39**, 3741 (1989).

[25] C. C. Huang, G. Nounesis, and D. Guillon, Phys. Rev. A **33**, 2602 (1986).

[26] R. Mahmood, M. Lewis, D. Johnson, and V. Surrendranath, Phys. Rev. A **38**, 4299 (1988).

[27] A. J. Jin *et al.*, Phys. Rev. E **53**, 3639 (1996).

[28] G. Iannacchione, E. Gorecka, W. Pyzuk, S. Kumar, and D. Finotello, Phys. Rev. E **51**, 3346 (1995).

[29] J. W. Goodby and R. Pindak, Mol. Cryst. Liq. Cryst. **75**, 233 (1981); see also C. C. Huang, Phys. Rev. A **28**, 2433 (1983).

[30] G. Nounesis, R. Geer, H. Y. Liu, C. C. Huang, and J. W. Goodby, Phys. Rev. A **40**, 5468 (1989).

[31] T. Pitchford, G. Nounesis, D. Dumrongrattana, J. M. Viner, C. C. Huang, and J. W. Goodby, Phys. Rev. A **32**, 1938 (1985).

[32] J. M. Viner, D. Lamey, C. C. Huang, R. Pindak, and J. W. Goodby, Phys. Rev. A **28**, 2433 (1983); G. Nounesis, C. C. Huang, and J. W. Goodby, Phys. Rev. Lett. **56**, 1712 (1986).

[33] T. Pitchford *et al.*, Phys. Rev. A **34**, 2422 (1986).

[34] G. Nounesis, Ph.D. thesis, University of Minnesota, 1990 (unpublished).

[35] W. Pyzuk, E. Gorecka, J. Szydlowska, A. Krowczynski, D. Pociecha, and J. Przedmojski, Phys. Rev. E **52**, 1748 (1995).

[36] D. Pociecha, E. Gorecka, A. Krowczynski, J. Szydlowska, and J. Przedmoojski (private communication).

[37] D. J. Bergman and B. I. Halperin, Phys. Rev. B **13**, 2145 (1976); see also M. A. deMoura, T. C. Lubensky, Y. Imry, and A. Aharony, *ibid.* **13**, 2176 (1976).

[38] R. Bruinsma and D. R. Nelson, Phys. Rev. B **23**, 402 (1981).